

PAPER • OPEN ACCESS

## A novel control strategy for enhancing the LVRT and voltage support capabilities of DFIG

To cite this article: Yangwu Shen *et al* 2018 *IOP Conf. Ser.: Earth Environ. Sci.* **121** 042035

View the [article online](#) for updates and enhancements.

### You may also like

- [Investigation of a converter fault for a DFIG wind turbine and analysis of the resulting gearbox component loads](#)  
Julian Röder, Georg Jacobs, Dennis Bosse et al.
- [Current source converter-based optimal power extraction and power control of a doubly fed induction generator \(DFIG\) using backstepping control](#)  
Ram Krishan Kumar and Jayanti Choudhary
- [A Control Methodology of Doubly Fed Induction Generator for Wind Energy Generation](#)  
M Pandikumar



**ECS**  
The  
Electrochemical  
Society  
Advancing solid state &  
electrochemical science & technology

**DISCOVER**  
how sustainability  
intersects with  
electrochemistry & solid  
state science research

# A novel control strategy for enhancing the LVRT and voltage support capabilities of DFIG

Yangwu Shen<sup>1</sup>, Bin Zhang, Liqing Liang and Ting Cui

State Grid Hunan Electric Power Corporation Research Institute, Changsha, Hunan, 410007, China

<sup>1</sup> shenyangwu@126.com

**Abstract.** A novel integrated control strategy is proposed in this paper to enhance the low voltage ride through capacity for the double-fed induction generator by equipping an energy storage system. The energy storage system is installed into the DC-link capacitor of the DFIG and used to control the DC-link voltage during normal or transient operations. The energy storage device will absorb or compensate the power difference between the captured wind power and the power injected to the grid during the normal and transient period, and the grid side converter can be free from maintaining the voltage stability of the DC-link capacitor. Thus, the grid-side converter is changed to reactive power support while the rotor-side converter is used to control the maximum power production during normal operation. The grid-side converter and rotor-side converter will act as reactive power sources to further enhance the voltage support capability of double-fed induction generator during the transient period. Numerical Simulation are performed to validate the effectiveness of the proposed control designs.

## 1. Introduction

As one of the most promising approaches to solve the energy crisis, wind power harnessing techniques have been under extensive studies in the new century[1]. With the increased wind power penetration, Modern grid codes require that the wind generator system can not only survive during external faults, but also have the capabilities of contributing to the network transient voltage support.

For many wind farm, doubly-fed induction generator (DFIG)based wind turbines are used. However, DFIG is very sensitive to grid disturbances, especially those causing the sudden drop of the DFIG terminal voltage. During such a fault, the DFIG may be disconnected from the grid to protect its rotor-side converter (RSC) and dc-link capacitor from damage because of the emergence of over-current in the rotor circuit and overvoltage in the dc-link capacitor. Hence, the conventional crowbar circuit which directly short circuits the rotor during grid fault via an external resistor is commonly suggested to protect the DFIG[1-14]. Despite the fact that the crowbar method is comparatively simple yet reliable, its weakness is also apparent, e.g. loss of the controllability of the stator active and reactive power and consumption of a large amount of reactive power during the fault period.

To cure the drawbacks of the crowbar protection, some control strategies on the rotor-or grid-side converter have been employed to protect the converters of DFIG. For example, the demagnetization methods in [6-8] and the feed-forward compensation strategy in [5] helped the DFIG ride through faults while its transient dynamics were still under control. Other advance control strategies [9] also have been proposed to enhance the LVRT capability of DFIG. Furthermore, many hardware-aided



methods have been developed [10-14], such as the rotor-side series dynamic resistances [10], the series GSC (SGSC) [11], DVR [12], energy storage device (ESD) [13], and nine-switch GSC [14]. Although an improved LVRT performance has been obtained using the existing methods in the literature, little concern has been given to transient reactive power control of the DFIG.

In this paper, by equipping ESS into the DFIG, a novel integrated control strategy of LVRT capability and reactive power support capability adapted to different depth of voltage sag for DFIG-ESS is proposed to improve the dynamic performance of such DFIG-ESS system during the grid fault. The organization of this paper is as follow. In Section 2, the topology of DFIG incorporated with ESS is briefly introduced. In Section 3, the methodology of DFIG LVRT enhancement with ESS is discussed. The reactive power control strategy and the controller design for the DFIG-ESS are present in Section 4. Case studies are described in Section 5. Section 6 concludes this paper.

## 2. Topology of DFIG incorporated with ESS

The structure of a wind power generator integrated with ESS is shown in Figure 1. In conventional configurations, the ESS and the switches connected to the DC-link are absent. The RSC is used to keep the maximum available wind power production and regulate the stator voltage, while the GSC is just responsible for regulating the DC-link voltage.

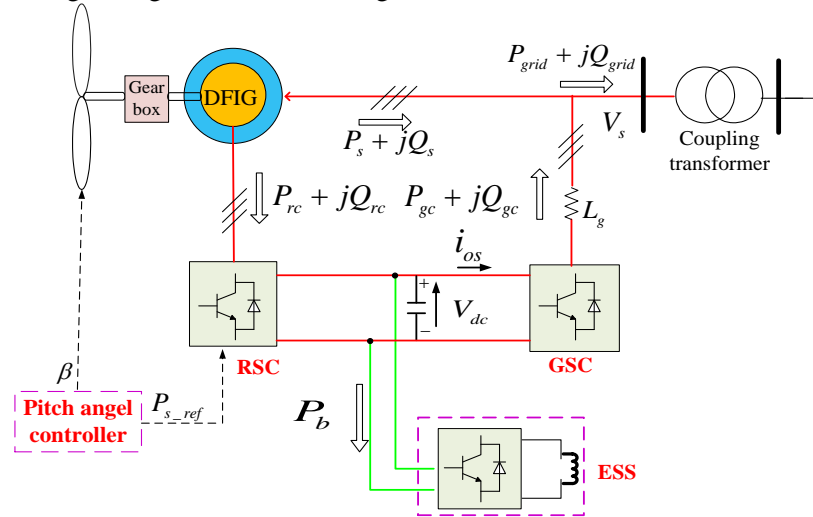


**Figure 1.** Structure of DFIG-ESS.

If the stator and rotor copper losses are neglected, the amount and the power flow direction through the rotor circuit can be approximately expressed as:

$$P_{rc} = P_w - P_s \quad (1)$$

Where  $P_w$ ,  $P_{rc}$ , and  $P_s$  represent the capture wind power, rotor power, and stator power, respectively. Normally, the power flow flocking into the rotor circuit ( $P_{rc}$ ) equals 20%~30% of the captured wind power ( $P_w$ ) during the normal operation at the super-synchronous operation. When the power grid is subject to a short-circuit fault, the transmitting capability of active power  $P_{rc}$  is extremely restricted due to the supply voltage drops. Consequently, it can be seen from (1) that the large transient wind power flows into the DC-link capacitor through the rotor circuit due to the low response of the generator and wind turbine, especially when the DFIG suffers a serious voltage drop.

According to the reference direction of different power shown in figure 1, the instantaneous dynamic response of the DC-link capacitor without ESS can be described as:

$$C v_{dc} \frac{dv_{dc}}{dt} = P_{rc} - P_{gc} = P_{rc} - e_{gd} i_{gd} = \Delta P \quad (2)$$

Where  $P_{gc}$  is the instantaneous input power of the GSC.  $e_{gd}$  and  $i_{gd}$  are the d-axis components of the grid voltage and current respectively.

For the traditional DFIG, the main task of GSC is to maintain the DC-link voltage level and provide a path for the rotor power to/from the grid. Hence, the DC-link capacitor could be protected. The adequate voltage on the rotor could be provided. However, it is difficult to realize that  $\Delta P$  in (2) equals zero when  $e_{gd}$  drops to a low value[7]. This is because the rotor power is large and the instantaneous power  $e_{gd}i_{gd}$  is small and determined by the current limitation of the converter semiconductor  $i_{g\max}$ . Therefore, the excessive power  $\Delta P$  cannot be transmitted to the power grid.

By adding an ESS and its converter to the DC-link, equation(2) can be rewritten as:

$$P_c = CV_{dc} \frac{dV_{dc}}{dt} = P_{rc} - P_b - P_{gc} \quad (3)$$

Where  $P_b$  is the power absorbed by ESS.

By tuning appropriate control parameters of ESS, the left side of (3) is zero, which means the DC-link voltage can be maintained as a constant value. equation (3) can be represented as:

$$P_b = P_{rc} - P_{gc} = (P_w - P_s) - (P_{grid} - P_s) = P_w - P_{grid} \quad (4)$$

Where  $P_w$  and  $P_{grid}$  are the captured wind power and the active power injected to the grid by the DFIG, respectively.

It can be seen from (3) and (4) that the ESS can regulate the DC-link voltage by absorbing or compensating the power from/to rotor circuit during normal/fault operation, therefore, there is little risk of over-voltage in the DC-link capacitor even if the GSC is controlled to transfer zero active power to the grid. In addition, the absorbed power difference between  $P_{gc}$  and  $P_{rc}$  is essentially equal to those between  $P_w$  and  $P_{grid}$ . Consequently, the excessive power flock into the DFIG can be handled by the ESS, which is actually equivalent to regulate the transient DC-link voltage during grid fault. Furthermore, the oscillation of the current in the rotor and stator can be reduced since the variation of the DC-link voltage is suppressed. This will be verified by the simulation results in Section 5. Therefore, the ESS connecting to the DC-link can enhance the LVRT capacity of the DFIG during voltage dips.

### 3. Reactive power control strategy and controller design for the DFIG-ESS

The transient response of DFIG-ESS varies with the different depth of voltage dips. Therefore, different control strategies can be designed for DFIG according the depth of the voltage dip. The flow chart of the integrate LVRT and enhanced reactive power support scheme is shown in figure 2. As can be seen in figure 2, three-layer control strategy of DFIG is proposed according to the magnitude of the supply voltage during fault period and different control strategies of GSC, RSC, and pitch angle control are designed for different layers.

The ESS is responsible for the DC-link voltage regulation during the normal and fault operations. When the supply voltage drops below 0.9 p.u., the RSC is used to control the maximum power production of the stator, while the GSC operates at the reactive power before participating into the voltage support. As the voltage drops between 0.75 p.u. and 0.5 p.u., the GSC acts as a reactive power source to inject the reactive power to the grid. The RSC is controlled to realize the LVRT capability and helps the GSC further enhance the reactive power capability of the DFIG under fault conditions. When the supply voltage suffers a serious voltage drop, (e.g., below 0.5 p.u.), the whole capacities of RSC and GSC are used to deliver the reactive power to the grid to boost the AC voltage. Furthermore, an auxiliary transient pitch angle controller is proposed to protect the rotor and realize the LVRT capability of DFIG.

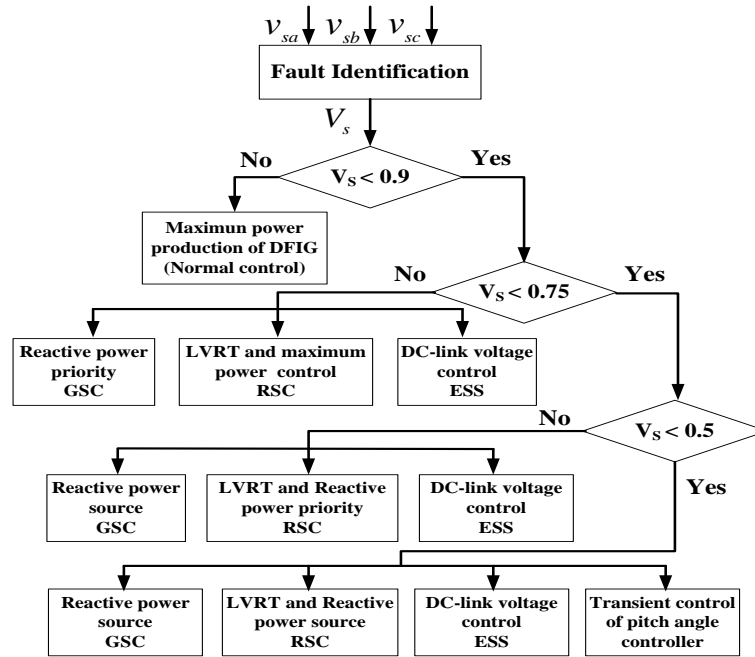


**Figure 2.**Flow chart of the integrated LVRT and enhancement reactive power support scheme.

#### A. Grid faults identification

In order to rapidly switch the normal controllers to the LVRT controllers, a good monitoring of the supply voltage dip is a crucial issue in the implementation of the proposed control strategy for the DFIG. In this paper, a sequence component decomposition method is implemented to detect the magnitude of the supply voltage.

#### B. Control strategy of ESS

The ESS can be readily integrated into the design of the DFIG by using a two-quarter IGBT-based DC/DC converter as depicted in figure 1. The control objective of the ESS is to regulate the DC-link voltage by keeping the power balance between RSC and GSC to make a good performance for the DFIG during normal and fault operations. figure 3 shows the overall vector control scheme of the ESS. The control strategy uses cascade control, whereby slower outer control loops regulate d- and q-axis current reference set point and inner faster current loops regulate the current tracking the reference current.

#### C. Controller and reactive power control strategy of GSC

The GSC can be free from managing the DC-link voltage since ESS is responsible for DC-link voltage regulation. The control strategy is applied here to modify the active power outer loop of the GSC, where the output active power of DFIG is regulated to the command value that comes from the system operator. It can also provide a limited reactive power support. Normally, the reference reactive power can be set to zero for the unity power factor operation. T

Based on (4), the relation between current of RSC ( $i_{or}$ ), current of GSC ( $i_{os}$ ) and current of ESS ( $i_b$ ) can be derived as:

$$i_b = i_{or} - i_{os} = i_{or} - \frac{\sqrt{3}m}{2\sqrt{2}} i_{gd} \quad (5)$$

Where  $m$  is the factor of the PWM modulation depth.

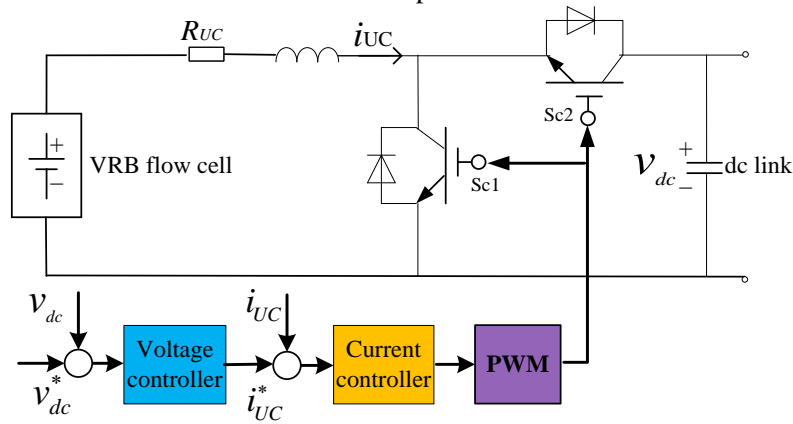


**Figure 3.** Configuration and control block diagram of bidirectional Buck-Boost DC/DC converter.

It is known from (5) that ESS maintains the DC-link voltage constant. This is also equivalent to regulate the current balance between  $i_{or}$  and  $i_{os}$ . If the controller of ESS is fast enough, the DC-link voltage can be kept constant even if  $i_{os}$  or  $i_{gd}$  reduces to zero. This reserves considerable potential reactive current capacity for GSC to participate into the voltage support during voltage sags. Therefore, it is proposed that the GSC can be contributed to the voltage support by injecting 4% reactive current for 1% supply voltage drop when the supply voltage falls below 0.9 p.u. to satisfy the requirement of grid codes, while the residual current capacity of GSC is used to deliver the active current to the grid. Figure 4 shows the coordinated control strategy of  $i_{gq}$  and  $i_{gd}$  for GSC during grid faults under the rated power active production condition as this is the most onerous situation that can be experience by a wind turbine. The control strategy with slight modification can meet the regulation of the other scenario.

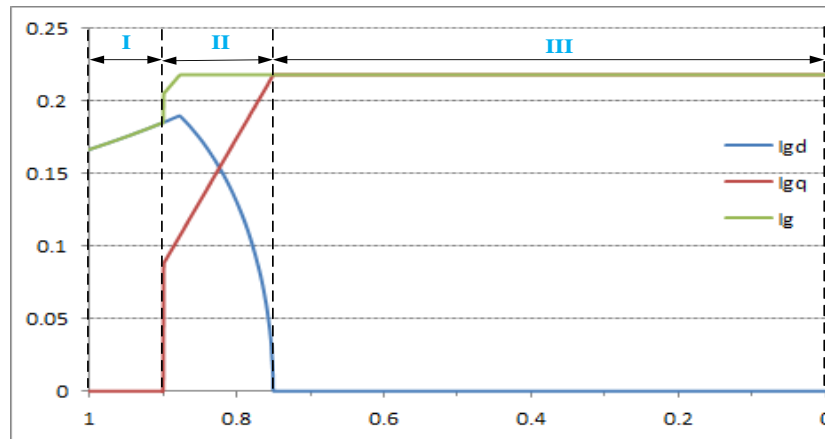


**Figure 4.** The coordinated active and reactive current control strategy for GSC.

Three different operation stages are observed in figure 4. In Stage I,  $i_{gd}$  increase from initial value of 0.17p.u., while  $i_{gq}$  maintains zero to deliver its rated active power at the unity power factor as the supply voltage drops from 1 p.u. to 0.9 p.u.. As the supply voltage continues to drop below 0.9 p.u. in Stage II,  $i_{gq}$  starts to linearly increase from 0.4 p.u. by 4% for each 1% reduction in the supply voltage magnitude.  $i_{gd}$  must decrease so that the grid current is constrained within the limits of semiconductor switches to ensure that  $|I_G| \leq 1$ . Consequently, the active power output of GSC is partially sacrificed for



the sake of the reactive power injection. Finally, when the supply voltage drops to 0.75 p.u.,  $i_{gq}$  equals 1.0 p.u. and  $i_{gd}$  reduces to zero, which means that the GSC acts as a reactive power source. The power flowing into the rotor circuit is completely absorbed by ESS.

For the GSC, the dynamic response of outer power control loop is slower than that of the inner current control loop. Thus, a single inner current control loop is proposed to provide a fast initial reactive current injection following the voltage drop, which can help to fulfill dynamic demanding requirements.

#### D. Controller and reactive power control strategy of RSC

In the normal mode, the RSC is used to extract the maximum available wind power and regulate the stator voltage (reactive power) in a decoupled manner. The dual-loop controls of torque-current and reactive power-current are applied in q- and d-axis, respectively. The independent control of the stator active power ( $P_s$ ) and reactive powers ( $Q_s$ ) can be achieved through regulating the q-axis current ( $i_{rq}$ ) and d-axis current ( $i_{rd}$ ) of the rotor current, given by:

$$\begin{cases} P_s = |V_s| \times i_{rq} \\ Q_s = |V_s| i_{rd} - \frac{|V_s|^2}{\omega L_s} \end{cases} \quad (6)$$

Normally,  $i_{rq}$  equals 75% of the current capacity of the RSC when DFIG extracts rated power at the unity power factor.  $P_s$  can be kept constant by increasing  $i_{rq}$  to compensate the voltage dip during the fault condition. Therefore, it is proposed that the DFIG works at the rated power production when the magnitude of voltage remains between 0.75 p.u. and 1 p.u.

When the voltage drops below 0.75 p.u., the output power of the stator seriously decreases since the current of RSC reaches its limitation. This leads to a significantly instantaneous imbalance between the incoming power from the wind and the power flowing into the grid. It has been analyzed above that the key point to realize the LVRT is to reduce the imbalance flocked into the DFIG during grid faults. The imbalance power can be reduced by decreasing the captured wind power, which can be achieved by increasing the generator speed to make the operation mode of DFIG shift to the non-optimal operation.

The electrical torque  $T_e$  can be expressed as a function of q-axis current of RSC, given by:

$$T_e = -\frac{L_m \Psi_s}{L_s} i_{rq} \quad (7)$$

One can easily deduce that the reduction of electrical torque can be obtained by reducing the active current ( $i_{rq}$ ). The imbalance torque between the electrical torque  $T_e$  and the mechanical torque  $T_m$  causes the acceleration of the generator speed and consequently reduces the captured wind power. Besides, the increase of the rotor speed converts the partial wind energy into the rotor kinetic energy, which further reduces the imbalance power flowing through the DFIG. Therefore, the transient over-current is not induced. The DFIG can keep the continuous operation during grid faults. Moreover, the reduction of  $i_{rq}$  during fault conditions reserves considerable potential reactive power capacity for the RSC to participate into the voltage control. It further enhances the voltage support capability of GSC which is limited as the voltage drops to a low value.

In order to meet the reactive power requirement by the stringent grid code, the RSC changes into the reactive current priority where the  $i_{rd}$  increases by 4% for 1% drop of the supply voltage amplitude while  $i_{rq}$  reduces to make the rotor current constrained within the limits of the RSC.

### E. Pitch angle controller

The relation between the angular rotor speed, the captured wind power, and the output power of DFIG can be expressed:

$$w_r^2 = \int \frac{2}{J} (P_w - P_g) dt \quad (8)$$

This formulation shows the generator speed decreases due to the decrease of  $P_w$ . Compared to the generator speed, the increase of pitch angle has a more significant impact on the reduction of the aerodynamic power extraction. Generally, the mechanical servo system is able to change the pitch angle of the blades at a rate around  $10^\circ/\text{sec}$ . It indicates that the pitch angle can be only altered several degrees during the grid fault transient (0.6~1s). For a given wind speed, if the blade pitch angle increases from  $0^\circ$  to  $10^\circ$ , the power coefficient drops from 0.48 to around 0.20 in a second. Consequently, the captured wind power decreases around 30%.

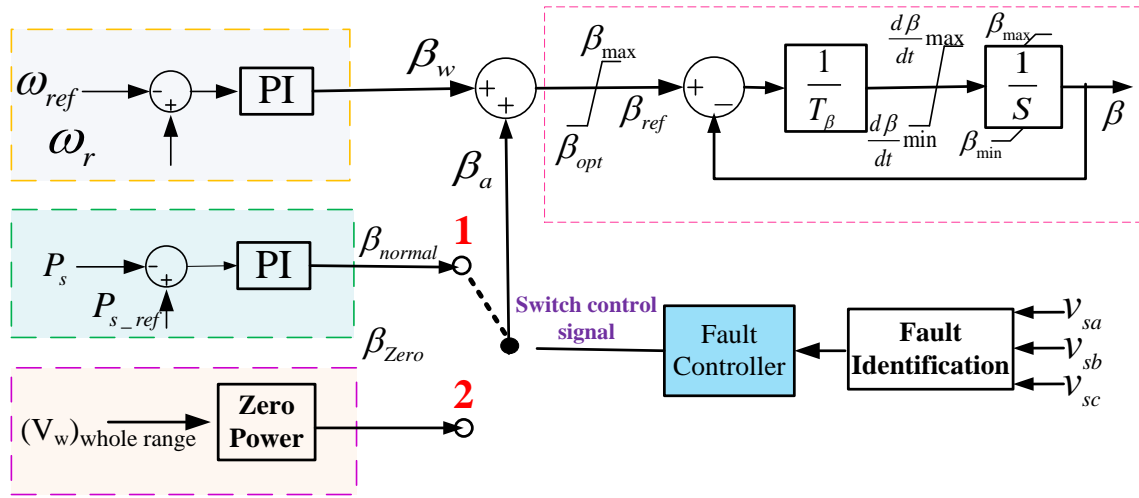


**Figure 5.** Improved pitch angle controller.

For the conventional PI controller, the wind turbine blade pitch angle is not controlled until the upper generator speed or rated power is reached. Therefore, it cannot effectively help reduce the captured wind power. It can be seen from (11) that if the captured wind power is reduced as soon as possible, the maximum generator speed will be significantly decreased. Consequently, the maximum generator speed and the over-current after fault clearance are seriously suppressed. Therefore, an auxiliary improved pitch angle controller (as shown in figure 5) is proposed to control the turbine blade pitch angle at the instant of voltage dips, when the generator speed is below the rated speed.

The switcher works at position 1 in the normal operation to prevent over-rated power production under high speed winds. As the amplitude of the supply voltage is below a certain threshold (0.5 p.u.), the fault controller is triggered to change the switcher to position 2. Thus, the pitch angle increases at the maximum rate to the desired value which is obtained from the Zero Power Block storing the pitch angle values corresponding to zero power output of the turbine over the whole range of wind speeds.

## 4. Simulations

In this section, simulations are carried out on a single-machine-infinite-bus system with a 1.5 MW DFIG based wind farm (as showed in Figure 6) to validate the proposed method in enhancing the LVRT capability of the DFIG as well as supporting the terminal voltage during grid faults.



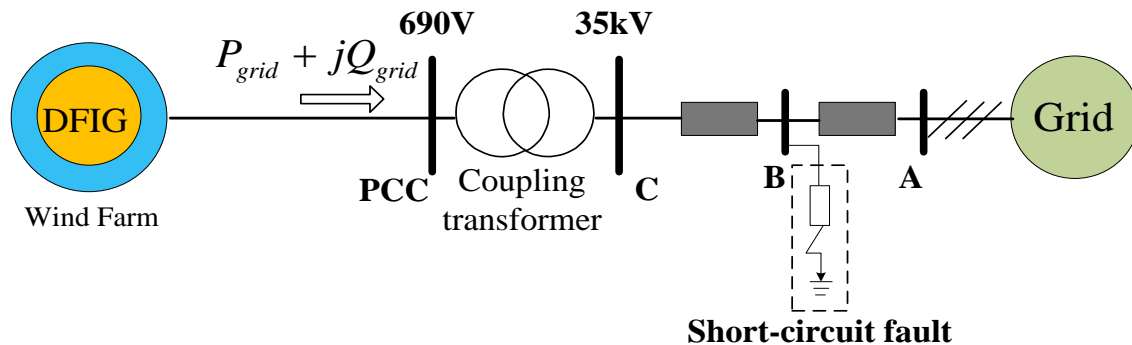


**Figure 6.** Schematic diagram of the tested system.

Two cases are performed as follows:

**Case 1:** examining the LVRT capability of the DFIG-ESS with the proposed control strategy during serious voltage dips;

**Case 2:** investigating the reactive power support capability of DFIG-ESS during medium-level voltage dips.

#### 4.1. LVRT capabilities of the DFIG with serious voltage drops

Besides the case where the proposed method (Method A) is used, the convention crowbar protection (Method B) is also employed during grid faults to give comprehensive comparisons. For the crowbar protection, the resistor is chosen to be 0.5 p.u.. The crowbar threshold is set to 1.5 times of the rated current. Note that the DC-chopper which is usually installed with the crowbar circuit in Method B is not used here, in order to investigate the capability of the ESS in controlling the DC-link voltage.

The RSC is controlled to extract the rated power and maintain zero reactive power output of the stator during the normal operation, which is corresponding to the super-synchronous operation mode of DFIG. A three-phase 85% supply voltage drop of 625 ms duration is assumed to occur at bus B at  $t=2s$ .

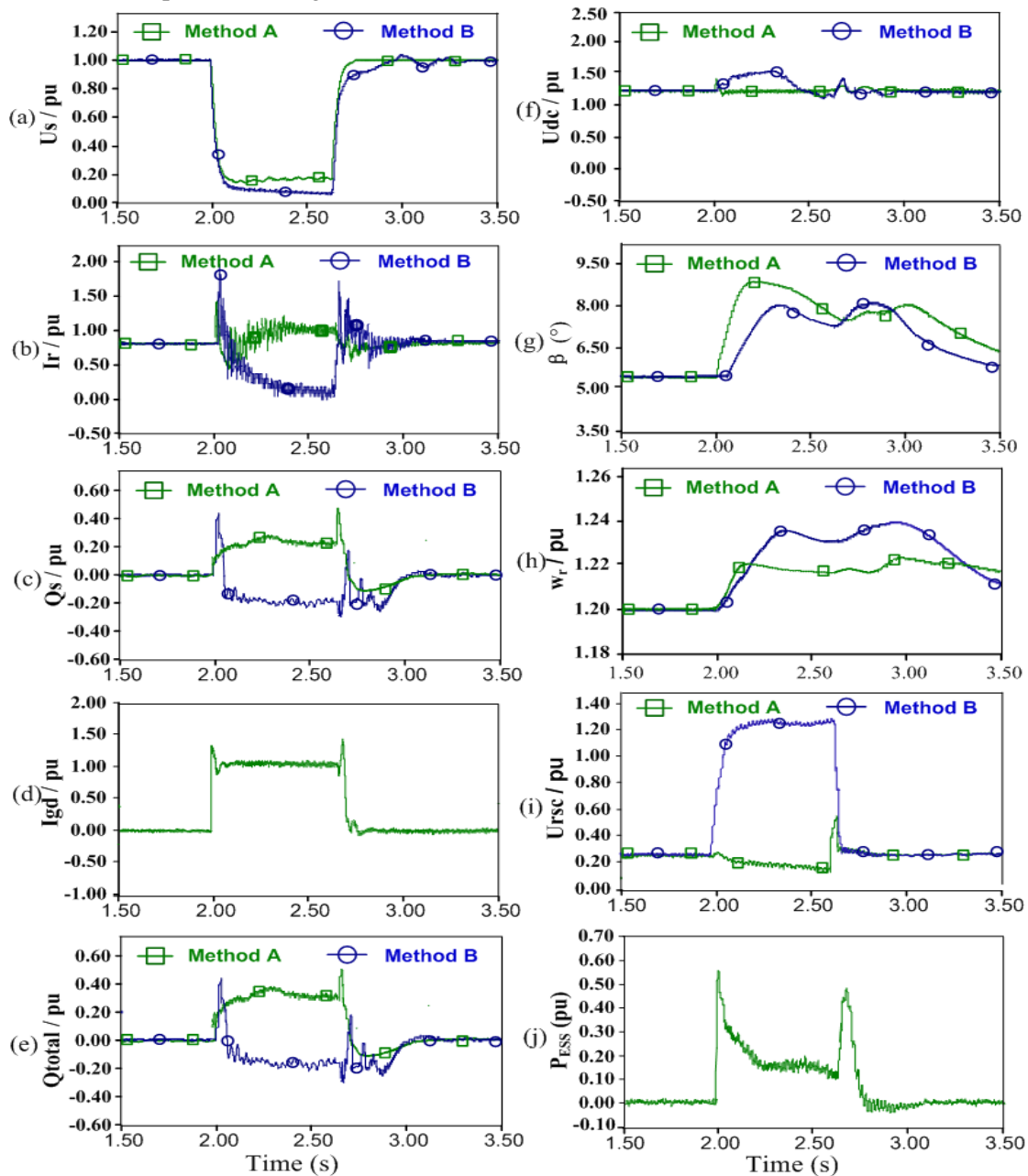
The transient behaviors of the DFIG with two different control strategies A and B are depicted in figure 7. It is observed that the transient behaviors in the case of Method A are better than those in the case of Method B. The rotor current and DC-link are suppressed below the crowbar threshold with Method A [see figure 7 (a) and (f)]. The DFIG can keep the continuous operation without the interruption of the crowbar and participate into the voltage support by injecting the reactive power to the grid [see figure 7(c)-(e)]. However, the DFIG with Method A starts to draw the reactive power from the grid [see figure 7(c)]. This reactive power consumed by the DFIG further reduces the voltage of the DFIG stator terminals to 0.1 p. u., as shown in figure 7(a). This is not acceptable when considering the grid codes. In addition, Method A can response much faster to increase the pitch angle than Method B. It indicates that less unbalance power flows into rotor and less power is stored in the rotor inertia energy. Consequently, the voltage on RSC, the maximum generator speed, and the stator and rotor current after fault clearance in Method A are less than those in Method B.

#### 4.2. Reactive power support capability of DFIG-ESS during voltage dips

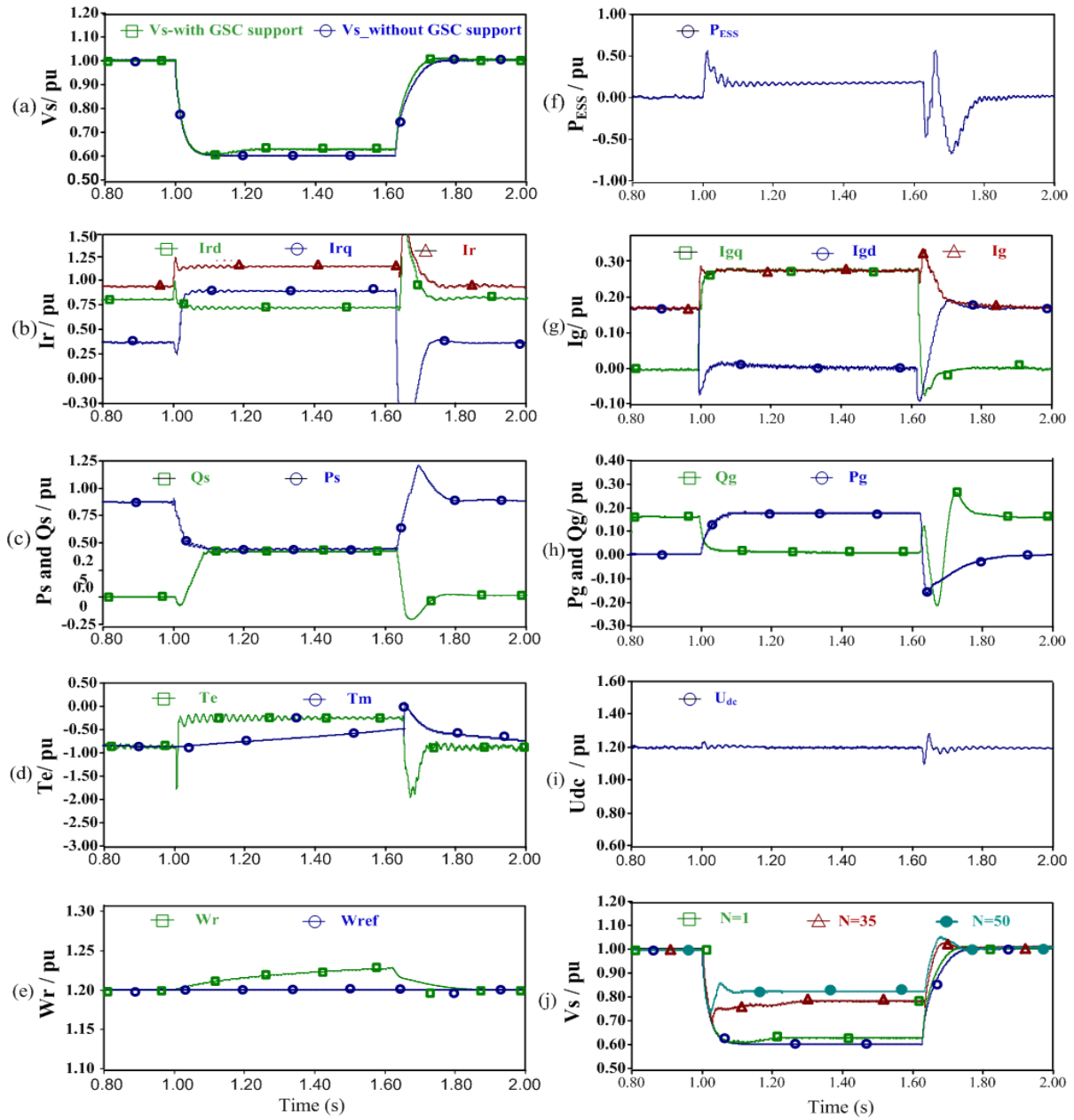
This simulation test is used to further verify the reactive power support capability of DFIG-ESS during grid voltage sags. The operations of the RSC and GSC are the same as those in Case 1. Bus B occurs a 625 ms three phase fault with remnant voltage of 0.6 p.u.. figure 8 shows the system response of the DFIG-ESS with the reactive power support priority scheme.

Figure 8(b) shows reactive power priority of DFIG-ESS during voltage dips. It is obvious that the priority of the RSC gives the reactive current to support the supply voltage recovery as the fault occurs. The reactive current increases from 0.33 p.u. to 0.90 p.u., while the active current decreases from 0.83 p.u. to 0.70 p.u.. The current of RSC is constrained within its limitation. As a result, the reactive power increases to 0.45 p.u., while the active power reduces from 0.83 p.u. to 0.45 p.u. [see figure 8(c)]. The reduction of the active current causes the decrease of the electromagnetic torque, which results in

gradual increase of the rotor speed from 1.20 to 1.22p.u.. However, this is not serious. Furthermore, the GSC acts as a reactive power source to boost the supply voltage [see figure 8(f) and (g)], since the rotor power can be handled by the ESS [see figure 8(e)]. Therefore, there is no risk of voltage stability for the DC-link capacitor [see figure 8(h)].



**Figure 7.** Transient responses of the DFIG-ESS with Method A and B: (a) terminal voltage, (b) rotor current, (c) reactive power output of the stator, (d) reactive current of the GSC, (e) total reactive power output of the DFIG, (f) DC-link voltage, (g) pitch angle, (h) rotor speed, (i) voltage of the RSC, and (j) active power of the ESS.



**Figure 8.** Reactive power priority of DFIG-ESS during voltage dips: (a) terminal voltage, (b) current of RSC, (c) output power of the stator, (d) electromagnetic and mechanical torque, (e) generator speed, (f) active power of the ESS, (g) current of GSC, (h) output power of the GSC, (i) DC-link voltage, and (j) terminal voltage with different amount of DFIG.

Generally, the improvement by Method A in the nadir part of the voltage is limited when the wind farm is simulated by only one DFIG. The provided reactive power is limited [figure 8(a)]. However, it is clear in figure 8(j) that such voltage enhancement becomes increasingly obvious as the number of the DFIG increases. Therefore, the promising prospects of applying the proposed method to large scale wind farms are confirmed for the voltage support during grid faults.

## 5. Conclusions

This paper developed a novel integrated control strategy to enhance the low voltage ride-through (LVRT) capacity for the doubly-fed induction generator (DFIG) by installing the energy storage

system (ESS). The reactive power supporting capability was also adapted to different depth of voltage sags for the DFIG-ESS to improve the dynamic performance during the grid fault. The ESS was connected to the DC-link capacitor of the DFIG and used to regulate the DC-link voltage during normal or fault operations. The unbalanced power between the captured wind power and the power injected to the grid during the transient process was absorbed or compensated by the ESS. The effectiveness of the proposed method was verified by simulation results on a single-machine-infinite-bus system.

## References

- [1] M Cui, D Ke, Y Sun, D Gan, J Zhang, and B-M Hodge 2015 Wind power ramp event forecasting using a stochastic scenario generation method *IEEE Trans. Sustain. Energy* **6**(2) 422–433
- [2] L H Yang, Z Xu, J Østergaard, Z Y Dong, and K P Wong 2008 Advance control strategy of DFIG wind turbines for power system fault ride through *IEEE Trans. Power Syst* **23**(2) 545–554
- [3] J Yao, H Li, Z Chen, X Xia, X Chen, Q Li, and Yong Liao, 2013 Enhanced control of a DFIG-based wind-power generation system with series grid-side converter under unbalanced grid voltage conditions *IEEE Trans. Power Electron.* **28**(7) 3167–3181
- [4] X Yan, G Venkataramanan, Y Wang, Q Dong, and B Zhang, 2011 Grid-fault tolerant operation of DFIG wind turbine generator using a passive resistance network *IEEE Trans. Power Electron* **26**(10) 2896–2905
- [5] J Liang, W Qiao, and R G Harley 2010 Feed-forward transient current control for low-voltage ride-through enhancement of DFIG wind turbines *IEEE Trans. Energy Convers* **25**(3) 836–843
- [6] S Hu, X Lin, Y Kang, and X Zou 2011 An improved low-voltage ride through control strategy of doubly fed induction generator during grid faults *IEEE Trans. Power Electron.* **26**(12) 3653–3665
- [7] D W Xiang, L Ran, P J Tavner, and S C Yang, 2006 Control of a doubly fed induction generator in a wind turbine during grid fault ride-through *IEEE Trans. Energy Convers* **21**(3) 652–662
- [8] S Xiao, G Yang, H Zhou, and H Geng, 2013 A LVRT control strategy based on flux linkage tracking for DFIG-based WECS *IEEE Trans. Ind. Electron.* **60**(7) 2820–2834
- [9] M J Hossain, T K Saha, N Mithulannanthan, and H R Pota, 2013 Control strategies for augmenting LVRT capability of DFIGs in interconnected power system,” *IEEE Trans. Ind. Electron.* **60**(6) 2510–2522
- [10] J Yang, J Fletcher, and J O’Reilly 2010 A series-dynamic-resistor-based converter protection scheme for doubly-fed induction generator during various fault conditions,” *IEEE Trans. Energy Convers.* **25**(2) 422–432
- [11] P S Flannery and G Venkataramanan 2009 Unbalanced voltage sag ride through of a doubly fed induction generator wind turbine with series grid-side converter,” *IEEE Trans. Ind. Appl.* **45**(5) 1879–1887
- [12] J Nielsen and F Blaabjerg, “A detailed comparison of system topologies for dynamic voltage restorers,” 2005 *IEEE Trans. Ind. Appl.* **41**(5) 1272–1280
- [13] C Abbey and G Joos, 2007 Supercapacitor energy storage for wind energy applications 2007 *IEEE Trans. Ind. Appl.* **43**(3) 769–776
- [14] P Kanjiya, B B Ambati, and V Khadkikar 2014 A novel fault-tolerant DFIG based wind energy conversion system for seamless operation during grid faults,” *IEEE Trans. Power Syst.* **29**(3) 1296–1305